REPORT

SEISMOLOGY

# Global quieting of high-frequency seismic noise due to COVID-19 pandemic lockdown measures

Thomas Lecocq[1]*, Stephen P. Hicks[2], Koen Van Noten[1], Kasper van Wijk[3], Paula Koelemeijer[4], Raphael S. M. De Plaen[5], Frédérick Massin[6], Gregor Hillers[7], Robert E. Anthony[8], Maria-Theresia Apoloner[9], Mario Arroyo-Solórzano[10], Jelle D. Assink[11], Pinar Büyükakpınar[12,13], Andrea Cannata[14,15], Flavio Cannavo[15], Sebastian Carrasco[16], Corentin Caudron[17], Esteban J. Chaves[18], David G. Cornwell[19], David Craig[20], Olivier F. C. den Ouden[11,21], Jordi Diaz[22], Stefanie Donner[23], Christos P. Evangelidis[24], Läslo Evers[11,21], Benoit Fauville[25], Gonzalo A. Fernandez[26], Dimitrios Giannopoulos[27,28], Steven J. Gibbons[29], Társilo Girona[30], Bogdan Grecu[31], Marc Grunberg[32], György Hetényi[33], Anna Horleston[34], Adolfo Inza[35], Jessica C. E. Irving[34,36], Mohammadreza Jamalreyhani[37,13], Alan Kafka[38], Mathijs R. Koymans[11,21], Celeste R. Labedz[39], Eric Larose[17], Nathaniel J. Lindsey[40], Mika McKinnon[41,42], Tobias Megies[43], Meghan S. Miller[44], William Minarik[45,46], Louis Moresi[44], Víctor H. Márquez-Ramírez[5], Martin Möllhoff[20], Ian M. Nesbitt[47,48], Shankho Niyogi[49], Javier Ojeda[50], Adrien Oth[51], Simon Proud[52], Jay Pulli[53,38], Lise Retailleau[54,55], Annukka E. Rintamäki[7], Claudio Satriano[54], Martha K. Savage[56], Shahar Shani-Kadmiel[21], Reinoud Sleeman[11], Efthimios Sokos[57], Klaus Stammler[23], Alexander E. Stott[58], Shiba Subedi[33], Mathilde B. Sørensen[59], Taka'aki Taira[60], Mar Tapia[61], Fatih Turhan[12], Ben van der Pluijm[62], Mark Vanstone[63], Jerome Vergne[64], Tommi A. T. Vuorinen[7], Tristram Warren[65], Joachim Wassermann[43], Han Xiao[66]

Human activity causes vibrations that propagate into the ground as high-frequency seismic waves. Measures to mitigate the coronavirus disease 2019 (COVID-19) pandemic caused widespread changes in human activity, leading to a months-long reduction in seismic noise of up to 50%. The 2020 seismic noise quiet period is the longest and most prominent global anthropogenic seismic noise reduction on record. Although the reduction is strongest at surface seismometers in populated areas, this seismic quiescence extends for many kilometers radially and hundreds of meters in depth. This quiet period provides an opportunity to detect subtle signals from subsurface seismic sources that would have been concealed in noisier times and to benchmark sources of anthropogenic noise. A strong correlation between seismic noise and independent measurements of human mobility suggests that seismology provides an absolute, real-time estimate of human activities.

Seismometers record signals from more than just earthquakes: Interactions between the solid Earth and fluid bodies, such as ocean swell and atmospheric pressure (*1*, *2*), are now commonly used to image and monitor the subsurface (*3*). Human activity is a third source of seismic signal. Nuclear explosions and fluid injection or extraction result in impulsive signals, but everyday human activity is recorded as a near-continuous signal, especially on seismometers in urban environments. These complicated signals are the superposition of a wide variety of activities happening at different times and places at or near Earth's surface but are typically stronger during the day than at night, weaker on weekends than weekdays, and stronger near population centers than sparsely inhabited areas (*4*–*7*). Seismometers in urban environments are important to maximize the spatial coverage of seismic networks and to warn of local geologic hazards (*8*), even though anthropogenic seismic noise degrades their capability to detect transient signals associated with earthquakes and volcanic eruptions. Therefore, it is vital to understand urban seismic sources, but studies have been limited to confined areas or distinct events, such as road traffic (*9*, *10*), public transport (*7*, *11*), and "football quakes" (*11*, *12*). Broad analysis of the long-term global anthropogenic seismic wavefield has been lacking. The impact of large, coherent changes in human behavior on seismic noise is unknown, as is how far it propagates and whether seismic recordings offer a coarse proxy for monitoring human activity patterns. Answering these questions has proven challenging because datasets are large, monitoring networks are heterogeneous, and the many possible noise sources likely vary spatially and overlap in time (*13*).

The coronavirus disease 2019 (COVID-19) outbreak was declared a global health emergency in January 2020 (*14*) and a pandemic in March 2020 by the World Health Organization. The outbreak resulted in emergency measures to reduce the basic reproduction rate of the virus (*15*), beginning in China and Italy and then followed by most countries. These measures disrupted social and economic behavior (*16*), industrial production (*17*), and tourism (*18*). In this paper, we use the term "lockdown" to



[1]Seismology-Gravimetry, Royal Observatory of Belgium, Brussels, Belgium. [2]Department of Earth Science and Engineering, Imperial College London, London, UK. [3]Department of Physics, University of Auckland, New Zealand. [4]Department of Earth Sciences, Royal Holloway University of London, Egham, UK. [5]Centro de Geociencias, Universidad Nacional Autónoma de México, Campus Juriquilla, Querétaro, Mexico. [6]Swiss Seismological Service, ETH Zurich, Zurich, Switzerland. [7]Institute of Seismology, University of Helsinki, Helsinki, Finland. [8]Albuquerque Seismological Laboratory, U.S. Geological Survey, Albuquerque, NM, USA. [9]Zentralanstalt für Meteorologie und Geodynamik (ZAMG), Vienna, Austria. [10]Escuela Centroamericana de Geología, Universidad de Costa Rica, San José, Costa Rica. [11]R&D Seismology and Acoustics, Royal Netherlands Meteorological Institute (KNMI), De Bilt, Netherlands. [12]Kandilli Observatory and Earthquake Research Institute, Boğaziçi University, Istanbul, Turkey. [13]GFZ German Research Centre for Geosciences, Potsdam, Germany. [14]Dipartimento di Scienze Biologiche, Geologiche e Ambientali, Università Degli Studi di Catania, Catania, Italy. [15]Istituto Nazionale di Geofisica e Vulcanologia, Osservatorio Etneo, Catania, Italy. [16]Bensberg Observatory, University of Cologne, Cologne, Germany. [17]Université. Grenoble Alpes, Université Savoie Mont Blanc, CNRS, IRD, IFSTTAR, ISTerre, Grenoble, France. [18]Volcanological and Seismological Observatory of Costa Rica at Universidad Nacional (OVSICORI-UNA), Heredia, Costa Rica. [19]Department of Geology and Geophysics, School of Geosciences, University of Aberdeen, King's College, Aberdeen, UK. [20]Dublin Institute for Advanced Studies, Geophysics Section, Dublin, Ireland. [21]Department of Geoscience and Engineering, Delft University of Technology, Delft, Netherlands. [22]Geosciences Barcelona, CSIC, Barcelona, Spain. [23]Federal Institute for Geosciences and Natural Resources (BGR), Hannover, Germany. [24]Institute of Geodynamics, National Observatory of Athens, Athens, Greece. [25]Noise Department, Brussels Environment, Brussels-Capital Region, Belgium. [26]Observatorio San Calixto, La Paz, Bolivia. [27]Seismotech S.A., Athens, Greece. [28]Laboratory of Geophysics & Seismology, Department of Environmental & Natural Resources Engineering, Hellenic Mediterranean University, Chania, Greece. [29]Norges Geotekniske Institutt, Oslo, Norway. [30]Geophysical Institute, University of Alaska Fairbanks, Fairbanks, AK, USA. [31]National Institute for Earth Physics, Magurele, Romania. [32]Réseau National de Surveillance Sismique (RENASS), Université de Strasbourg, CNRS, EOST UMS830, Strasbourg, France. [33]Institute of Earth Sciences, Faculty of Geosciences and Environment, University of Lausanne, Lausanne, Switzerland. [34]School of Earth Sciences, University of Bristol, Queen's Road, Bristol, UK. [35]Instituto Geofisico del Peru, Lima, Peru. [36]Department of Geosciences, Princeton University, Princeton, NJ, USA. [37]Institute of Geophysics, University of Tehran, Tehran, Iran. [38]Weston Observatory, Department of Earth and Environmental Sciences, Boston College, Weston, MA, USA. [39]Seismological Laboratory, California Institute of Technology, Pasadena, CA, USA. [40]Geophysics Department, Stanford University, Stanford, CA, USA. [41]SETI Institute, Mountain View, CA, USA. [42]Faculty of Science, Department of Earth, Ocean and Atmospheric Sciences, University of British Columbia, Vancouver, BC, Canada. [43]Ludwig-Maximilians-Universität München, Munich, Germany. [44]Research School of Earth Sciences, Australian National University, Canberra, ACT, Australia. [45]Department of Earth and Planetary Sciences, McGill University, Montréal, QC, Canada. [46]GEOTOP Research Centre, Montréal, QC, Canada. [47]Raspberry Shake, S.A., Boquete, Chiriqui, Panama. [48]Department of Earth and Climate Science, University of Maine, Orono, ME, USA. [49]University of California, Riverside, CA, USA. [50]Departamento de Geofísica, Universidad de Chile, Santiago, Chile. [51]European Center for Geodynamics and Seismology, Walferdange, Grand Duchy of Luxembourg. [52]National Centre for Earth Observation, Department of Physics, University of Oxford, Oxford, UK. [53]Raytheon BBN Technologies, Arlington, VA, USA. [54]Université de Paris, Institut de Physique du Globe de Paris, Paris, France. [55]Observatoire Volcanologique du Piton de la Fournaise, Institut de Physique du Globe de Paris, La Plaine des Cafres, France. [56]School of Geography, Environment and Earth Sciences, Victoria University of Wellington, Wellington, New Zealand. [57]Department of Geology, University of Patras, Patras, Greece. [58]Department of Electrical and Electronic Engineering, Imperial College London, South Kensington Campus, London, UK. [59]Department of Earth Science, University of Bergen, Bergen, Norway. [60]Berkeley Seismological Laboratory, University of California Berkeley, Berkeley, CA, USA. [61]Laboratori d'Estudis Geofísics Eduard Fontserè, Institut d'Estudis Catalans (LEGEF-IEC), Barcelona, Spain. [62]Department of Earth and Environmental Sciences, University of Michigan, Ann Arbor, MI, USA. [63]Geology Department, Truro School, Truro, Cornwall, UK. [64]Institut de Physique du Globe de Strasbourg, UMR 7516, Université de Strasbourg/EOST, CNRS, Strasbourg, France. [65]Department of Physics, University of Oxford, Oxford, UK. [66]Department of Earth Science and Earth Research Institute, University of California, Santa Barbara, CA, USA.
*Corresponding author. Email: thomas.lecocq@seismology.be

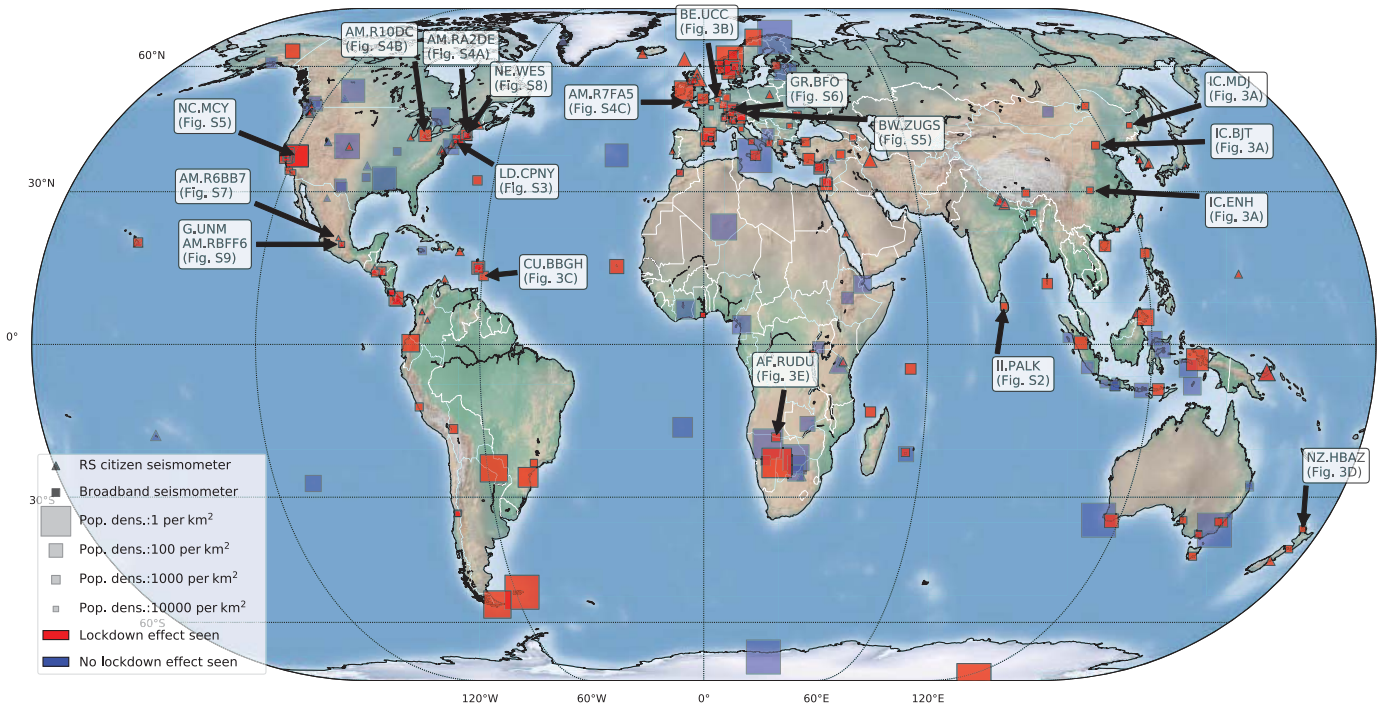


**Fig. 1. Locations of analyzed seismic stations throughout the world.** The map shows locations of the 268 global seismic stations with usable data (e.g., no long data gaps, working sensors) that we analyzed. Lockdown effects were observed (red) at 185 of 268 stations. Symbol size is scaled by the inverse of population density (*30*) to emphasize stations located in remote areas. The labeled stations are discussed in detail in the text.

broadly encompass many types of emergency measures, such as full quarantine [e.g., in Wuhan, China (*19*–*21*)], enforced physical distancing (e.g., in Italy and the United Kingdom), travel restrictions (*22*), widespread closure of services and industry, and any other emergency measures. These major changes to daily life provide an opportunity to study their environmental impacts, such as reductions in nitrous oxide emissions in the atmosphere (*23*). Recordings of human-generated seismic vibrations that travel through the solid Earth provide insights into the dynamics of pandemic lockdowns.

We assessed the effects of COVID-19 lockdowns on high-frequency (4 to 14 Hz) seismic ambient noise (hiFSAN) (*24*). We compiled a global seismic noise dataset using vertical-component seismic waveform data from 337 broadband and individually operated citizen seismometer stations (*24*), such as Raspberry Shake instruments (RSs), with a self-noise well below the ground motion generated by anthropogenic noise (*25*) and flat responses in the target frequency band (Fig. 1). We obtained usable data (e.g., no large data gaps, working sensors) from 268 stations and detected pronounced reductions in hiFSAN during local lockdown measures at 185 stations (Fig. 2). Periods that are often seismically quiet include weekends, as well as the Christmas and New Year holidays for locations where they are celebrated. Notably, we found a near-global reduction in noise, commencing in China in late January 2020 (*26*), followed by Italy (*26*, *27*), the whole of Europe, and the rest of the world in March to April 2020. This period of reduced noise lasted longer and was often quieter than the Christmas–to–New Year period.

In China (Fig. 3A), the COVID-19 outbreak and subsequent emergency measures occurred during the Chinese New Year (CNY). In Enshi, a city located in Hubei province where the outbreak began (*28*), hiFSAN in 2020 clearly diverged from the normal annual reduction during CNY. The hiFSAN level remained at a minimum, demarcated by the start and end of quarantine in Hubei, for several weeks after CNY. Although the quarantine measures in Beijing were less strict, local hiFSAN reductions were more pronounced and lasted longer than in recent years. As of the end date of our analysis, Beijing has still not reached the average hiFSAN level of previous years, which suggests that the impact of COVID-19 is continuing to restrict anthropogenic noise there. We noticed a later hiFSAN lockdown reduction in April 2020 in Heilongjiang (Fig. 3A), in northeast China, near the Russian border.

Although we observed seismic effects of lockdown in areas with low population density estimates (<1 person per $km^2$; Fig. 1), the strongest hiFSAN reduction occurred in populated environments. For a permanent seismic station in Sri Lanka, a 50% reduction in hiFSAN occurred after lockdown, which is the strongest we observed in the available data from that station since at least July 2013 (fig. S2). In Central Park, New York, on Sunday nights, hiFSAN was 10% lower during the lockdown than before this period (fig. S3).

Seismic networks in populated areas enable us to correlate hiFSAN with other human activity measurements, such as audible recordings and flight data (*24*). At a surface station in Brussels, Belgium (Fig. 3B), we found a 33% reduction in hiFSAN after lockdown. We compared this noise level with data from a nearby microphone, located close to a major road, that mainly records audible traffic noise. We found a high correlation between prelockdown hiFSAN and audible noise, both showing characteristic diurnal and weekly changes. However, during lockdown, audible noise reductions were more pronounced, which suggests that seismometers are sensitive to a wide distribution of seismic sources, not just nearby traffic. Audible and hiFSAN levels then gradually increased after April 2020. Independent mobility data (*24*) provide insights into what caused these changes. Mobility correlates with hiFSAN at lockdown, with correlation coefficients >0.8 (*24*), except for time spent at places of residence (Google's "residential" category), which is expected given the increased number of people spending more time at home because of government restrictions.

Citizen seismometers provide a different urban ground motion dataset, with denser coverage in some places. Large hiFSAN drops

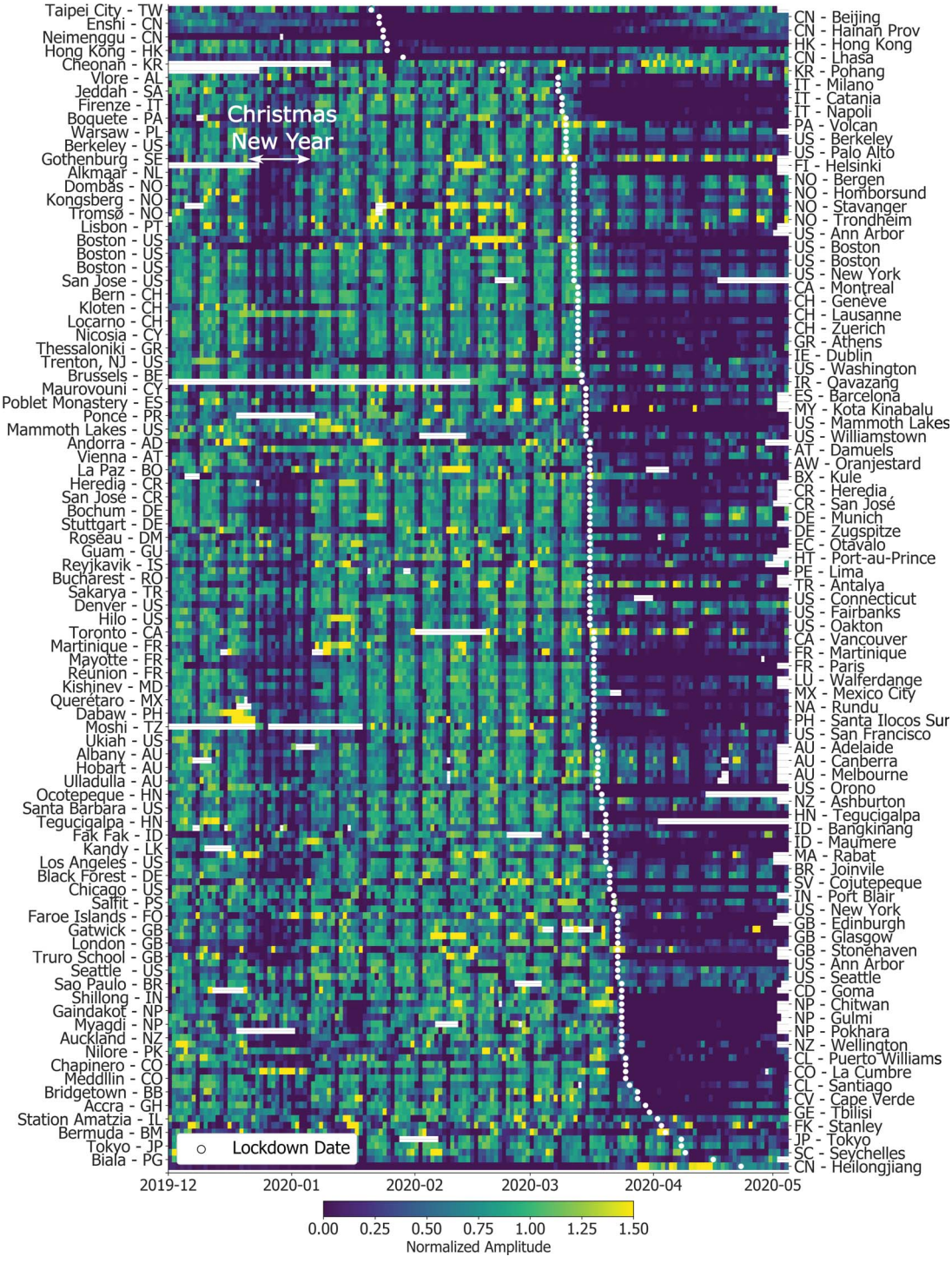


**Fig. 2. Global temporal changes in seismic noise.** Global daily median hiFSAN is depicted (*24*), normalized to percentage variation of the baseline before lockdown measures and sorted by lockdown date. Each line of the image corresponds to one seismic station. Data gaps are shown in white. Location and country code are indicated for each station; see fig. S1 for network and station codes.

occurred particularly at schools and universities after lockdown-related closures [e.g., in Boston and Michigan (United States) and Cornwall (United Kingdom); fig. S4]. The hiFSAN level was even 20% lower than during school holidays, which indicates sensitivity to the environment outside of the school.

The pandemic has also affected tourism—for example, during the holiday season in the Caribbean. In Barbados (Fig. 3C), hiFSAN decreased by ~45% after lockdown on 28 March 2020 through April 2020 and stayed ~50% below levels observed in previous years for the same period. However, seismic noise levels began to decrease 1 to 2 weeks before a local curfew was implemented. Local flight data (*24*) indicate that travel to Barbados started decreasing after 21 March 2020, and the overall reduction in hiFSAN might have been partly due to tourists repatriating. We also observed noise reductions due to decreased tourist activity at ski resorts in Europe (Zugspitze in Germany) and the United States (Mammoth Mountain in California) (fig. S5).

Although we observed lockdown effects most prominently at surface stations, we also detected them underground. In New Zealand, seismometers installed in boreholes (to minimize the effects of anthropogenic noise) monitor potential hazards associated with the Auckland

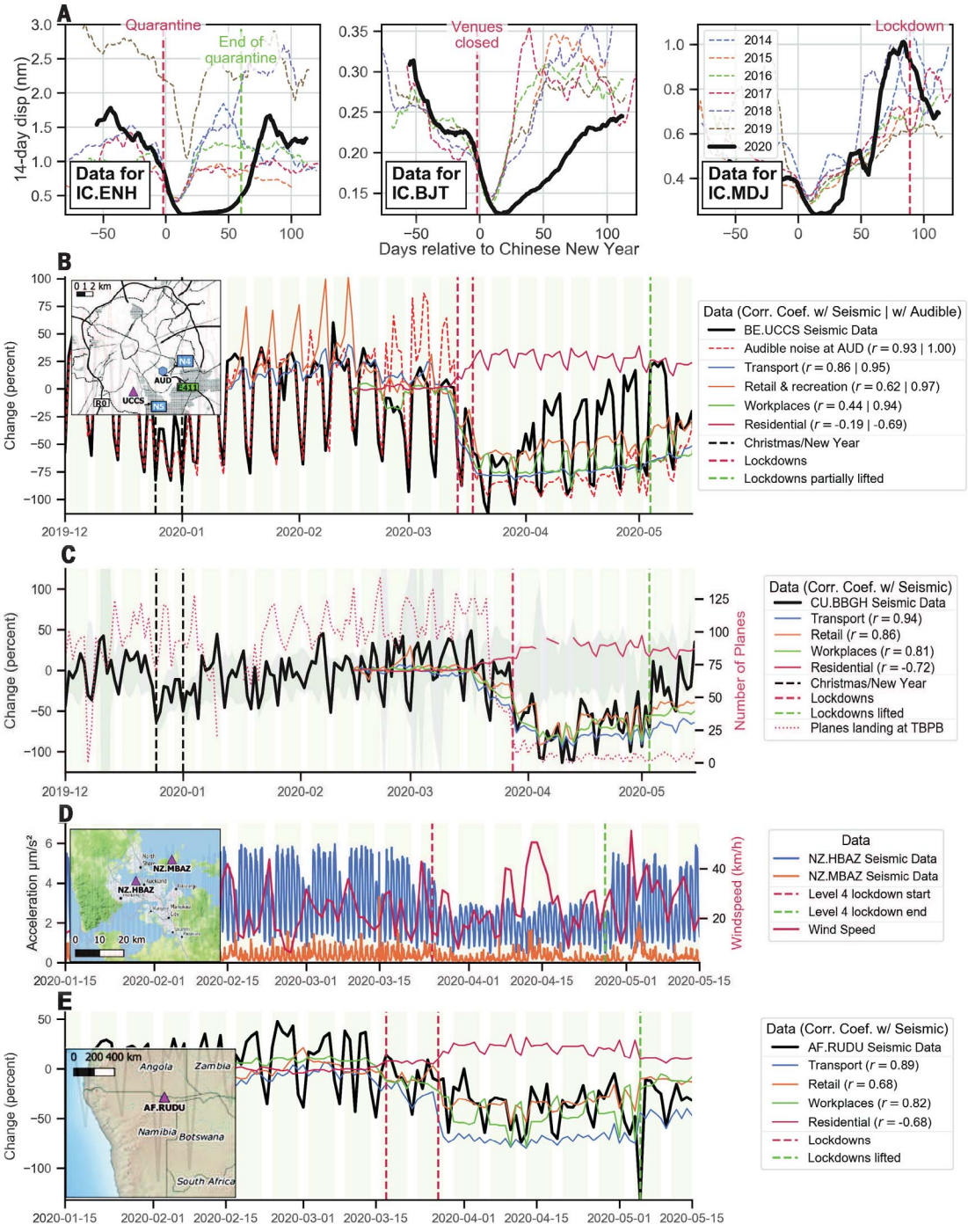


**Fig. 3. Regional examples of the 2020 seismic noise quiet period.** The examples show different features of the lockdown seismic signal changes in regional settings. We filtered the hiFSAN data between 4 and 14 Hz and present temporal changes as displacement (A), acceleration (D), or percentage change relative to the baseline before lockdown [(B), (C), and (E)], with the panels in (A) also relative to the baseline of corresponding time periods in previous years. Individual seismic stations are identified by codes in "network. station" format (IC.ENH, BE.UCCS, etc.). The keys in (B) to (E) include correlation coefficients (*r*) with mobility data (*24*). (**A**) Lockdown effects at three stations in China compared with the Chinese New Year holiday in previous years. (**B**) Lockdown effects on hiFSAN compared with audible environmental noise and independent mobility data in Brussels, Belgium. (**C**) Lockdown effect in Barbados compared with noise levels of the past decade (gray shading) and correlation with local flight data at the Grantley Adams International Airport (TBPB) (*24*). (**D**) Lockdown noise reduction recorded on borehole seismometers in Auckland, New Zealand. (**E**) Lockdown noise reduction in a region of low population density in Rundu, Namibia.

Volcanic Field (*6*, *8*, *29*). Station HBAZ is 380 m below the city, whereas MBAZ is at 98 m of depth, 14 km from the city center on the uninhabited Motutapu Island (Fig. 3D). The hiFSAN level at both stations varied between weekdays and weekends before the lockdown, which suggests that both are sensitive to anthropogenic activity. Although the island station is quieter overall, the lockdown instigated a reduction in hiFSAN by a factor of 2 for both stations. We attribute the remaining hiFSAN maxima on the island (mid-April 2020 and early May 2020) to strong winds and high waves. On 27 April 2020, New Zealand lifted restrictions, with hiFSAN increasing to the prelockdown levels.

The reduction of hiFSAN was weaker in less populated areas such as Rundu, located along the Namibia-Angola border (Fig. 3E). After COVID-19 was confirmed in Namibia, an emergency was declared on 17 March 2020 to restrict mobility, followed by full lockdown on 27 March 2020. These measures are reflected in the >25% hiFSAN reduction compared with prelockdown levels. Despite Rundu having a population roughly one-eighth and one-fifth as dense as those of Brussels and Auckland, respectively (*30*), we observed a similarly high correlation between seismic and mobility data. The Black Forest Observatory in Germany is an even more remote station, located 150 to 170 m below the surface in crystalline bedrock. Although this station is considered a reference

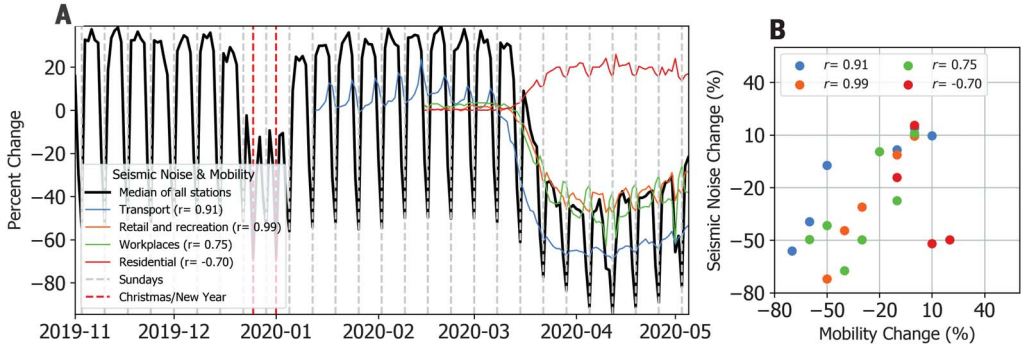


**Fig. 4. Global changes in seismic noise compared with population mobility trends.** (**A**) Comparison between temporal changes in global daily median hiFSAN based on data from the 185 stations that observed lockdown effects and population mobility changes (*24*). (**B**) Scatter plot to illustrate the correlation between the binned (10% bins) time series of seismic noise changes and all categories of mobility data in (A). Percentage changes are expressed relative to a prelockdown baseline. All categories show a strong positive correlation, apart from time spent in residential premises, which is anticorrelated.

laboratory with low noise overall (*31*), we detected a small hiFSAN reduction during lockdown nights (fig. S6), corresponding to the lowest hiFSAN since at least 25 December 2015.

Here we have provided a global-scale analysis of high-frequency anthropogenic seismic noise. Global median hiFSAN dropped by as much as 50% during March to May 2020 (Fig. 4). The length and quiescence of this period represent the longest and most coherent global seismic noise reduction in recorded history, emphasizing how human activities affect the solid Earth. A globally high correlation exists between changes in hiFSAN and population mobility (*24*), with correlations exceeding 0.9 for many categories.

This distinct low-noise period will help optimize seismic monitoring efforts (*4*). The ability to analyze the full spectrum of seismogenic behavior, including the smallest earthquakes, is essential for monitoring fault dynamics over seismic cycles, as well as for earthquake forecasting and seismic hazard assessment. Small earthquakes should dominate datasets (*32*), but typical operational catalogs using amplitude-based detection do not include many of the smallest earthquakes (*33*). This detection issue is especially problematic in populated areas, where anthropogenic noise energy interferes with earthquake signals. This problem is exemplified by recordings of a moment magnitude 5.0 earthquake at 15 km of depth southwest of Petatlan, Mexico, during lockdown (fig. S7). An earthquake with this magnitude and source mechanism that occurs during the daytime would typically be observed at stations in urban environments only if the signal was filtered. However, the reduction of seismic noise by ~40% during lockdown made this event visible, without any filtering required, at a RS station in Querétaro city, 380 km away. Low noise levels during COVID-19 lockdowns could thus allow detection of signals from previously unrecognized sources in areas with incomplete seismic catalogs. Such newly identified signals could be used as distinct templates (*32*) for finding similar waveforms in noisier data before and after lockdown. This approach also works for tremor signals that are masked by anthropogenic noise yet vital for monitoring potential volcanic unrest (*6*). Although broadband sensors in rural environments are less affected by anthropogenic noise, any densification of and reliance on low-cost sensors in urban areas, such as RSs and low-cost accelerometers (*34*), will require a better understanding of anthropogenic noise sources to suppress false detections. As populations increase globally, more people become exposed to potential natural and induced geohazards (*35*). Urbanization will increase anthropogenic noise in exposed areas, further complicating seismic monitoring efforts. The ability to characterize and minimize anthropogenic noise is becoming increasingly important for accurate detection and imaging of seismic signatures of potentially harmful subsurface hazards.

Anthropogenic seismic noise is thought to be dominated by noise sources <1 km away from detectors (*5*–*7*, *11*, *36*). Because population mobility generates time-varying loads that radiate energy through the shallow subsurface as Rayleigh waves (*11*), local effects such as construction sites and heavy machinery can affect individual stations. However, the 2020 seismic noise quiet period reveals that when considering multiple stations or whole networks over longer time scales, the anthropogenic seismic wavefield affects large areas. With denser networks and more citizen sensors in urban environments, additional features of the seismic noise, rather than just amplitude, will become usable and will help identify different anthropogenic noise sources (*10*, *37*). Characterizing these sources will be useful for imaging the shallow subsurface in three dimensions in urban areas by using high-frequency anthropogenic ambient noise (*38*, *39*). Our finding of a distributed noise field is supported by strong correlations with independent mobility data (Fig. 4). In contrast to mobility data, publicly available data from existing seismometer networks provide an objective absolute baseline of human activity levels. Therefore, hiFSAN can serve as a near–real-time technique for monitoring anthropogenic activity patterns, with fewer potential privacy concerns than those raised by mobility data collection. In addition, although industrial activities may not be captured in mobility data, they may produce a seismic noise signature. The 2020 seismic quiet period is a baseline for using seismic properties (*36*) to identify and isolate the sources contributing to the anthropogenic noise wavefield, especially when combined with data indicative of human behavior. Seismic observations of human activity during COVID-19 lockdowns have enabled us to assess the impact of mitigation policies—particularly the time to establish and recover from lockdowns—on daily life. As such, hiFSAN may provide important constraints for future health and behavioral science studies.

## REFERENCES AND NOTES


1. J. N. Brune, J. Oliver, *Bull. Seismol. Soc. Am.* **49**, 349–353 (1959).
2. R. K. Cessaro, *Bull. Seismol. Soc. Am.* **84**, 142–148 (1994).
3. N. M. Shapiro, M. Campillo, *Geophys. Res. Lett.* **31**, L07614 (2004).
4. D. E. McNamara, R. P. Buland, *Bull. Seismol. Soc. Am.* **94**, 1517–1527 (2004).
5. J. C. Groos, J. R. Ritter, *Geophys. J. Int.* **179**, 1213–1231 (2009).
6. C. M. Boese, L. Wotherspoon, M. Alvarez, P. Malin, *Bull. Seismol. Soc. Am.* **105**, 285–299 (2015).
7. D. N. Green, I. D. Bastow, B. Dashwood, S. E. Nippress, *Seismol. Res. Lett.* **88**, 113–124 (2017).
8. C. L. Ashenden *et al.*, *Nat. Hazards* **59**, 507–528 (2011).
9. N. Riahi, P. Gerstoft, *Geophys. Res. Lett.* **42**, 2674–2681 (2015).
10. N. J. Lindsey *et al.*, *Geophys. Res. Lett.* **47**, e2020GL089931 (2020).
11. J. Díaz, M. Ruiz, P. S. Sánchez-Pastor, P. Romero, *Sci. Rep.* **7**, 15296 (2017).
12. P. Denton, S. Fishwick, V. Lane, D. Daly, *Seismol. Res. Lett.* **89**, 1902–1907 (2018).
13. D. Wilson *et al.*, *Bull. Seismol. Soc. Am.* **92**, 3335–3342 (2002).
14. C. Sohrabi *et al.*, *Int. J. Surg.* **76**, 71–76 (2020).
15. R. M. Anderson, H. Heesterbeek, D. Klinkenberg, T. D. Hollingsworth, *Lancet* **395**, 931–934 (2020).
16. M. Nicola *et al.*, *Int. J. Surg.* **77**, 206–216 (2020).
17. T. Laing, *Extr. Ind. Soc.* **7**, 580–582 (2020).
18. A. Hoque, F. A. Shikha, M. W. Hasanat, I. Arif, A. B. A. Hamid, *Asian J. Multidiscip. Stud.* **3**, 52–58 (2020).
19. M. U. G. Kraemer *et al.*, *Science* **368**, 493–497 (2020).
20. H. Tian *et al.*, *Science* **368**, 638–642 (2020).
21. J. Zhang *et al.*, *Science* **368**, 1481–1486 (2020).
22. M. Chinazzi *et al.*, *Science* **368**, 395–400 (2020).
23. M. Bauwens *et al.*, *Geophys. Res. Lett.* **47**, 11 (2020).
24. Materials and methods and network citations are available as supplementary materials.

25. R. E. Anthony, A. T. Ringler, D. C. Wilson, E. Wolin, . *Seismol. Res. Lett.* **90**, 219–228 (2019).
26. H. Xiao, Z. C. Eilon, C. Ji, T. Tanimoto, *Sesimol. Res. Lett.* 10.1785/0220200147 (2020).
27. P. Poli, J. Boaga, I. Molinari, V. Cascone, L. Boschi, *Sci. Rep.* **10**, 9404 (2020).
28. H. Lau *et al*., *J. Travel Med.* **27**, taaa037 (2020).
29. S. Sherburn, B. J. Scott, J. Olsen, C. Miller, *N. Z. J. Geol. Geophys.* **50**, 1–11 (2007).
30. Center for International Earth Science Information Network CIESIN Columbia University, Gridded population of the world, version 4 (GPWv4): Population density. Revision 11, accessed 2 June 2020 (2018); https://doi.org/10.7927/H49C6VHW.
31. W. Zürn *et al*., *Geophys. J. Int.* **171**, 780–796 (2007).
32. B. Gutenberg, C. F. Richter, *Bull. Seismol. Soc. Am.* **34**, 185–188 (1944).
33. Z. E. Ross, D. T. Trugman, E. Hauksson, P. M. Shearer, *Science* **364**, 767–771 (2019).
34. E. S. Cochran, *Nat. Commun.* **9**, 2508 (2018).
35. G. J. H. McCall, *Geol. Soc. London Eng. Geol. Spec. Publ.* **15**, 309–318 (1998).
36. M. Lehujeur, J. Vergne, J. Schmittbuhl, A. Maggi, *Geotherm. Energy* **3**, 3 (2015).
37. G. Hillers, M. Campillo, Y.-Y. Lin, K.-F. Ma, P. Roux, *J. Geophys. Res.* **117**, B06301 (2012).
38. M. Picozzi, S. Parolai, D. Bindi, A. Strollo, *Geophys. J. Int.* **176**, 164–174 (2009).
39. F. Brenguier *et al*., *Geophys. Res. Lett.* **46**, 9529–9536 (2019).
40. T. Lecocq *et al*., ThomasLecocq/2020_Science_GlobalQuieting: First Release - v1.0, Zenodo (2020); https://doi.org/10.5281/zenodo.3944739.


## ACKNOWLEDGMENTS

We sincerely thank two anonymous reviewers, T. Nissen-Meyer, and J. Slate for their comments, which have improved the manuscript. We are extremely grateful to all seismic network managers, operators, and technicians who have helped facilitate the raw global seismic dataset (*24*). We also kindly acknowledge all of the passionate community seismologists for running their "home" seismometers and contributing, indirectly, to a better understanding of Earth. Any use of trade, firm, or product names is for descriptive purposes only and does not imply endorsement by the U.S. government. We dedicate this community-led study to all essential workers who have kept our countries going during these difficult times. **Funding:** P.K. was funded by a Royal Society University Research Fellowship (URF\R1\180377). P.B. and M.J. acknowledge support from the International Training Course "Seismology and Seismic Hazard Assessment" funded by the GeoForschungsZentrum Potsdam (GFZ) and the German Federal Foreign Office through the German Humanitarian Assistance program (grant S08-60 321.50 ALL 03/19). P.B. also acknowledges financial support from the Boğaziçi University Research Fund (BAP 15683). O.F.C.d.O acknowledges funding from a Young Investigator Grant from the Human Frontier Science Program (HFSP project RGY0072/2017). C.P.E. and E.S. acknowledge funding from the HELPOS Project "Hellenic Plate Observing System" (MIS 5002697). L.E. and S.S.-K. acknowledge funding from a VIDI project from the Dutch Research Council (NWO project 864.14.005). G.A.F. acknowledges contributions from the Observatorio San Calixto, which is supported by the Air Force Technical Application Center (AFTAC). C.R.L. acknowledges funding from the NSF Graduate Research Fellowship Program (grant DGE-1745301). V.-H.M. and R.D.P. acknowledge support from grant CONACYT-299766. R.D.P. acknowledges support from the UNAM-DGAPA postdoctoral scholarship. J.O. acknowledges support from the Agencia Nacional de Investigación y Desarrollo (Scholarship ANID-PFCHA/Doctorado Nacional/2020-21200903). S.P. acknowledges financial support from the Natural Environment Research Council (NE/R013144/1). A.E.R. acknowledges support from the K.H. Renlund foundation. M.K.S. acknowledges the New Zealand Earthquake Commission (EQC project 20796). H.X. acknowledges support from a Multidisciplinary Research on the Coronavirus and its Impacts (MRCI) grant from UC Santa Barbara. The Australian Seismometers in Schools data used in this research are supported by AuScope, enabled by the Australian Commonwealth NCRIS program. A.O. acknowledges support from the project RESIST, funded by the Belgian Federal Science Policy (contract SR/00/305) and the Luxembourg National Research Fund. **Author contributions:** T.L. designed and led the research. T.L., S.P.H., K.V.N., K.v.W., P.K., and R.S.M.D.P. processed and visualized the data and drafted the manuscript. F.M. contributed to the software development and provided the supplementary movie. G.H. thoroughly edited and reviewed the manuscript. All authors processed seismic data, took part in discussions, and performed a full interactive review of the original and revised manuscripts. **Competing interests:** The authors declare no competing interests. **Data and materials availability:** The raw data used to compute the hiFSAN were obtained from different networks and data providers (*24*). The computed data and codes used to analyze and plot Figs. 1 to 4 are available from the companion repository: https://github.com/ThomasLecocq/2020_Science_GlobalQuieting and (*40*).

## SUPPLEMENTARY MATERIALS

science.sciencemag.org/content/369/6509/1338/suppl/DC1
Materials and Methods
Supplementary Text
Figs. S1 to S9
Tables S1 to S3
References (*41*–*56*)
Movie S1

10 June 2020; accepted 14 July 2020
Published online 23 July 2020
10.1126/science.abd2438